Atmos. Meas. Tech. Discuss., 5, 7187–7222, 2012
www.atmos-meas-tech-discuss.net/5/7187/2012/
doi:10.5194/amtd-5-7187-2012

Atmospheric Measurement Techniques Discussions

A multi-year record of airborne CO_2 observations in the US Southern Great Plains

S. C. Biraud[1], **M. S. Torn**[1], **J. R. Smith**[2], **C. Sweeney**[3], **W. J. Riley**[1], **and P. P. Tans**[3]

[1]Lawrence Berkeley National Laboratory, Berkeley, California, USA
[2]Atmospheric Observing System Inc., Boulder, Colorado, USA
[3]NOAA Earth System Research Laboratory, Boulder, Colorado, USA

Received: 1 September 2012 – Accepted: 5 September 2012 – Published: 25 September 2012

Correspondence to: S. C. Biraud (SCBiraud@lbl.gov)

Published by Copernicus Publications on behalf of the European Geosciences Union.

Abstract

We report on 10 yr of airborne measurements of atmospheric CO_2 concentrations from continuous and flask systems, collected between 2002 and 2012 over the Atmospheric Radiation Measurement Program Climate Research Facility in the US Southern Great Plains (SGP). These observations were designed to quantify trends and variability in atmospheric concentrations of CO_2 and other greenhouse gases with the precision and accuracy needed to evaluate ground-based and satellite-based column CO_2 estimates, test forward and inverse models, and help with the interpretation of ground-based CO_2 concentration measurements. During flights, we measured CO_2 and meteorological data continuously and collected flasks for a rich suite of additional gases: CO_2, CO, CH_4, N_2O, $^{13}CO_2$, carbonyl sulfide (COS), and trace hydrocarbon species. These measurements were collected approximately twice per week by small aircraft (Cessna 172 first, then Cessna 206) on a series of horizontal legs ranging in altitude from 460 m to 5300 m (a.m.s.l.). Since the beginning of the program, more than 400 continuous CO_2 vertical profiles have been collected (2007–2012), along with about 330 profiles from NOAA/ESRL 12-flask (2006–2012) and 284 from NOAA/ESRL 2-flask (2002–2006) packages for carbon cycle gases and isotopes. Averaged over the entire record, there were no systematic differences between the continuous and flask CO_2 observations when they were sampling the same air, i.e. over the one-minute flask-sampling time. Applying the concept of broadband validation, we documented a mean difference of < 0.1 ppm between instruments. However, flask data were not equivalent in all regards; horizontal variability in CO_2 concentrations within the 5–10 min legs sometimes resulted in significant differences between flask and continuous measurement values for those legs, and the information contained in fine-scale variability about atmospheric transport was not captured by flask-based observations. The annual CO_2 concentration trend at 3000 m (a.m.s.l.) was 1.91 ppm yr^{-1} between 2008 and 2010, very close to the concurrent trend at Mauna Loa of 1.95 ppm yr^{-1}. The seasonal amplitude of CO_2 concentration in the Free Troposphere (FT) was half that in the PBL ($\sim$ 15 ppm

AMTD
5, 7187–7222, 2012

vs. ∼ 30 ppm) and twice that at Mauna Loa (approximately 8 ppm). The CO_2 horizontal variability was up to 10 ppm in the PBL and less than 1 ppm at the top of the vertical profiles in the FT.

1 Introduction

The steady rise and seasonal cycle of atmospheric CO_2 concentrations, first documented in detail at the Mauna Loa observatory (Keeling, 1960; Pales and Keeling, 1965) and now at systematic monitoring sites around the world has greatly contributed to our understanding of the carbon cycle and its relationship to a changing climate (Peters et al., 2010; Huntzinger et al., 2011). Nevertheless, uncertainties in the terrestrial carbon sink are among the greatest sources of uncertainty in predicting climate over the next century (NACP SIS, 2005; Friedlingstein et al., 2006; IPCC, 2007). In addition, for climate mitigation policy, there is a growing focus on testing and implementing methods for monitoring and verifying anthropogenic emissions (Mays et al., 2009; Shepson et al., 2011).

Atmospheric CO_2 concentration observations, combined with inverse modelling, can be used to estimate land and ocean CO_2 sources and sinks at regional and continental scales (Tans et al., 1990; Enting et al., 1995; Rayner et al., 1999; Gurney et al., 2002; Ciais et al., 2010). In addition, airborne and tall tower observations of atmospheric CO_2 mixing ratios are increasingly used to validate satellite-based or ground-based column CO_2 retrievals, test new airborne sensors (Abshire et al., 2010), and test the representativeness of ground-based observations (Xueref-Remy et al., 2011). Airborne campaigns with continuous CO_2 observations can also be used to investigate horizontal and vertical variability of CO_2 concentrations at multiple scales (Lin et al., 2004; Choi et al., 2008; Carouge et al., 2010).

However, there are many fewer airborne campaigns compared to the number of land-based towers observations, few vertical profiles relating Planetary Boundary Layer (PBL) and Free Troposphere (FT) concentrations, few measurement programs with

AMTD
5, 7187–7222, 2012

regular airborne observation missions, and poor uncertainty quantification (Hill et al., 2011). As a result, inversions are under-constrained (Ciais et al., 2010). As a results, publications on modelling of atmospheric transport (Peters et al., 2007; Pickett-Heaps et al., 2011) and CO_2 surface flux inferred from atmospheric inversions (Stephens et al., 2007; Ciais et al., 2010) called for more precise continental CO_2 concentration vertical profiles. There are also errors in inversion estimates due to uncertainty in CO_2 observations themselves (Rayner et al., 2002), and regions poorly constrained by the measurements (Gurney et al., 2004). Measurement errors have been assumed to be small, based on laboratory calibration and analysis of known concentrations in blind tests (Masarie et al., 2001). Another important source of error in inverse estimates is due to the very small concentration differences that must be resolved among observing sites to infer spatial gradients in CO_2 surface fluxes. For example, Stephens et al. (2011) estimated that ≤ 0.2 ppm differences between two observatories located 500 km apart must be resolved for a resolution of $\sim 50\,\mathrm{g\,C\,m^{-2}\,yr^{-1}}$ (for context, a annual NEE measured at SGP is typically around $-300\,\mathrm{g\,C\,m^{-2}\,yr^{-1}}$, Riley et al., 2009). Likewise, Marquis and Tans (2008) set a goal of ≤ 0.1 ppm comparability for measurements used in global atmospheric monitoring. Inter-laboratory differences assessed from round-robin comparison have shown that the uncertainty in measured CO_2 from several laboratories is approaching 0.10 ppm (WMO, 2011), and such comparability is becoming mainstream, thanks to the standardization of observational procedures and commercialization of new plug-and-play ground-based instruments developed by companies like LI-COr, Los Gatos Inc., Picarro Inc., and others. Nevertheless, the goal of ≤ 0.1 ppm has eluded aircraft-based observations because of the difficulty of ensuring high-accuracy measurements under changing ambient pressure and temperature in a mechanically stressed environment.

We designed our airborne program to provide a well documented data set able to meet the science needs identified above. Our high frequency vertical profiles from the Southern Great Plains (SGP) have proven useful to validate atmospheric CO_2 column measurements from ground-based Fourier transform spectrometer (Wunch et al.,

AMTD
5, 7187–7222, 2012

2010, 2011) and satellite-based retrievals (Kulawik et al., 2010, 2012; Kuai et al., 2012). The objectives of this paper are to: (1) demonstrate the concept of broadband validation for airborne observations and apply it to observations collected in the US Department Of Energy (DOE) Atmospheric Radiation Measurement (ARM) Climate Research Facility (ACRF) Southern Great Plains (SGP); (2) present results from a multi-year record of CO_2 observations to explore seasonal, vertical, and high frequency patterns in continuous CO_2 observations; and (3) provide documentation and uncertainty quantification to enable application of these observations to a broad set of researchers and research questions.

2 Methods

The ARM program supports a large testbed ($\sim 300 \times 300$ km) for measurements and modelling in the US Southern Great Plains (Ackerman et al., 2004). All atmospheric and climatic variables measured in the ACRF are available from the ARM Data Archives (www.arm.gov). The heart of the SGP site is the heavily instrumented Central Facility (CF) located at 36°37′ N, 97°30′ W, 314 m a.s.l. (a.m.s.l.), near the town of Lamont, Oklahoma. Forests dominate the eastern one-third of Oklahoma and the ACRF; the western half of the state is primarily agricultural and grassland. Spring and early summer is generally characterized by active weather patterns, with numerous frontal systems and precipitation. In contrast, fall is usually dry and sunny.

The Lawrence Berkeley National Laboratory (LBNL) ARM Carbon project started in 2001 with state-of-the-art CO_2 atmospheric concentration measurements (Bakwin et al., 1998) from a 60 m tower located at the CF and a system of fixed and mobile instruments for measuring CO_2, water, and energy fluxes, deployed at selected locations around the SGP region (Billesbach et al., 2004; Fischer et al., 2012). In 2002, airborne observations over the central facility started as part of a joint effort between the ARM program, the Earth System Research Laboratory (ESRL) of the US National Oceanic and Atmospheric Administration (NOAA), and the LBNL ARM Carbon project.

AMTD
5, 7187–7222, 2012

The focus of this project is to collect aerosol and trace-gas vertical profiles on board a small manned aircraft (Cessna 172). The typical flight pattern consisted of a series of 12 level legs at standard altitudes, ranging from 460 m to 5300 m (a.m.s.l.) centered over the 60 m CF tower (Fig. 1). Each leg was flown at constant altitude and lasted 5 (below 1800 m) or 10 (above 1800 m) minutes. Because of additional DOE restrictions on instrument flight rules, these flights had a strong daytime, clear-sky bias (Fig. 2). These observations were the first routine measurements in the world of atmospheric CO_2 profiles co-located with simultaneous ground continuous CO_2 flux and mixing ratios measurements (Pak et al., 1996; Langenfelds et al., 1999), and were for a time the only such measurements conducted routinely over the agricultural heartland of North America. Flask samples are analyzed by NOAA ESRL for a suite of carbon cycle gases and isotopes, thereby linking all flights to the global cooperative air-sampling network (http://www.esrl.noaa.gov/gmd/ccgg/flask.html). In 2006, the aircraft was upgraded to accommodate a larger payload (Cessna 206), and instrumentation for flask collection at 12 heights was added. In 2007, continuous CO_2 concentration measurements were initiated, making these the only routine, long-term, continuous CO_2 profile observations over the US In 2008, the airborne program expanded its scope and became a separate project: the ARM Airborne Carbon MEasurements Project (ACME). Data collected under this program can be accessed through the ARM web-based portal (http://www.arm.gov/campaigns/aaf2008acme). All CO_2 observations of this paper are reported in the WMO/GAW X2007 scale.

2.1 Flask-based observation methods

Starting in 2002, we collected bi-weekly flasks as part of the NOAA/ESRL Global Monitoring Division Aircraft Group. Flask samples were, and continue to be, analyzed in Boulder by the Carbon Cycle Greenhouse Gases group (CCGG) for CO_2, CH_4, CO, H_2, N_2O, and SF_6; and by the Institute of Arctic and Alpine Research (INSTAAR) for many Volatile Organic Compounds (VOCs) such as Acetylene (C_2H_2) and propane (C_3H_8). A pair of flasks (2 l each) was collected at a given altitude per flight, either in

AMTD
5, 7187–7222, 2012

the mid-PBL (~ 600 m), or in the FT (~ 3000 m). If the pair of flasks was collected in the mid-PBL, we tried to coordinate airborne sampling with ground flask sampling, yielding near-synchronous collection of samples at 60 m and 600 m. A total of 676 flasks were collected and analyzed between September 2002 and January 2006 with this system, leading to 334 pairs of observations. Among those pairs of flasks, 199 were collected in the FT and 135 were collected within the PBL (including 51 ground coordinated samplings).

The flask technology was upgraded in 2006. A 12-flask technology, designed by NOAA/ESRL was installed on the aircraft and has been used up to the present. With this technology, samples are collected at each horizontal leg of the vertical profile described in the section above. The flask sampler has two components: (1) a rack-mounted Precision Compressor Package (PCP) and (2) a Portable multi-Flask Package (PFP). Prior to each flight, the pilot connects a new PFP to the resident PCP. An automatic test is then performed to check for leaks and plumbing problems. The PCP is connected to a platform display that allows the pilot to trigger sampling when the desired location and altitude have been reached. For each sample, the inlet is first flushed with 5 l of ambient air; then the flask itself is flushed with 10 l of ambient air. After flushing of the inlet and flask is complete, the downstream valve of the flask is closed to achieve a 40 psia pressurization of the flask. After each flight, the filled PFP is returned to the NOAA laboratory for analysis of the suite of trace gases. As of July 2012, a total of 3868 flasks had been collected, constituting 332 vertical profiles. Due to infrastructure requirements for maintaining a large stock of operational PFPs and conducting the intensive analyses performed on the flask samples, we are currently collecting flask samples on only one out of every three-four flights.

2.2 Continuous CO_2 observation methods

In June 2007, a continuous NDIR CO_2 analyzer (hereafter referred to as RM0 for rack mount system #0), built by Atmospheric Observing System Inc. (AOS, Boulder Colorado), was deployed on the aircraft (Fig. 3) and has been used since. The core of the

AMTD
5, 7187–7222, 2012

system is a nickel-plated, differential aluminum analyzer and gas processor, designed around two identical nickel-plated gas cells, one for reference gas and the other for sample gas. Radiation sources are collimated through the gas cells, and then concentrated onto temperature controlled photo-detectors. Absorption of the radiation serves as the measure of CO_2 concentration. There are no moving parts, and the sources are modulated electronically at 8 Hz. A pair of identical radiation filters, one in front of and the other behind, each gas cell isolates radiation to the targeted molecular band centered at 4.26 µm with a width of 0.20 µm. The final piece of the analyzer is the custom digital demodulator which converts the differential AC signal generated by the analyzer into a DC response. The resulting DC signal is an averaged count of CO_2 concentration over a specified bandwidth (currently 8 Hz) reported in volts, and a corresponding sample dew point. The system controls flow rate, pressure, and valve switching. The remainder of the system consists of compressors, reference gases (called responsitivity, zero, and target in the text), an air drier (a combination of a semi-permeable membrane (Nafion)) followed by a cartridge of magnesium perchlorate), and electrical cables.

Forty five minutes before take-off, the pilot turns the system on by flipping a single power switch and operating three mechanical valves that enable air flow between the sub-systems and isolating the plumbing from outside air when it is not being used. The Analyzer operates autonomously during flight. The steps are reversed at the end of a mission. Data are typically downloaded within minutes after each flight. Reduction of each mission and decomposition into vertical profiles and transects are done in final form in about 10 min by a program developed and written by AOS, Inc. Additional software is used to track reference gas usage and diagnose pneumatic and electronic performances of the analyzer. The system is intended to be used to measure CO_2 in the atmosphere (350 ppm to 450 ppm range). It has negligible sensitivity to the motion of the platform. Typically, the air stream reaching the sample cell has a dew point of −55 °C, corresponding to less than 100 ppm water vapour.

During the warm-up cycle, the reference cell is flushed with differential zero gas (which is the only gas that cell ever sees) for two minutes at 0.2 slpm to make sure the

AMTD
5, 7187–7222, 2012

reference cell is dry (−55 °C dew point temperature) and fully flushed. After the first two minutes, the flow in the reference cell is alternatively turned down to no flow (for 20 s) or to a trickle flow (10 sccm for 3 min). During that time, the sample cell is flushed at 0.2 slpm with differential zero gas (for 20 s) or dried ambient air (for 3 min). This cycle is repeated 6 times. The warm-up phase ends with constant flushing of the sample cell with dried atmospheric ambient air for 11 min. The warm-up cycle, which consists of flushing the plumbing and both cells, takes about 45 min and needs to be completed prior to take-off. After the initial 45 min, the measurement cycle starts, consisting of calibration gas measurements (20 s), followed by 3 min sampling measurements. The calibration is a differential zero, a target, or a responsivity gas. Every fifth differential zero is alternatively replaced by either a responsivity or a target gas measurement (Fig. 4).

Regular Maintenance consists of: (1) replacing the magnesium perchlorate cartridge every 45 flight hours (about every 15 flights for our project) to minimize effects of water vapour; (2) recharging the reference gases every 240 flight hours (about every 80 flights for our project); and (3) verifying the calibration of the reference gases using 14 field-standards cylinders ranging from 350 to 450 ppm (WMO X2007 scale). As of March 2012, the original analyzer (RM0) has performed with an accuracy of 0.1 ppm at 1 Hz (including bias) for more than 329 missions (∼ 1000 flight hours). The calibration of the on-board cylinders (differential zero, responsivity, and target) is crucial and done when cylinders are installed in the analyzer system on the platform, i.e. in the field, replicating measurement conditions. To achieve this, field calibration cylinders are connected to a buffer volume (100 ml), vented to ambient pressure. Calibrating the machine at the inlet of the system (not only the analyzer) is important, accounting for all biases associated with the machine (drier, plumbing, analyzer itself).

2.3 Supporting data

Between 2002 and 2008, Relative Humidity (RH) and Temperature (T) vertical profiles were recorded continuously as part of the ARM In situ aerosol profiles (IAP) campaign.

AMTD
5, 7187–7222, 2012

Since 2008, RH and T profiles have been collected as part of the on-board ozone analyzer. Because these ancillary data are collected by independent data acquisition systems, we do not always have a full set of observations of RH, T, and continuous CO_2.

2.4 Precision and accuracy

Immediately after collection, each flask package is returned to NOAA/ESRL for analysis for as many as 55 trace gases. A non-dispersive infrared analyzer measures 100 ml of sample for CO_2 with a precision of ±0.03 ppm (Conway et al., 1994). The precision of the instrument is determined from 1 standard deviation of ~20 aliquots of natural air measured from a known cylinder. Note that flask-based observations have a documented bias of ~0.007 ppm per day of storage (http://www.esrl.noaa.gov/gmd/ccgg/aircraft/qc.html) due to differential diffusion of CO_2 through the Teflon O-ring sealing located at the end of each flask. This bias is not taken into account when flask-based measurements are reported. Considering that it takes on average about 3 weeks for a flask to be shipped to the sampling location, collected, and returned to the lab for analysis, there may be a storage offset of as much as 0.2 ppm.

On 16 March 2011 a second analyzer built by AOS (RM12), was deployed on the aircraft with an intentional 15 s plumbing delay relative to RM0. Except having an older, noisier generation of electronics, RM12 is very similar in operation to RM0. The two AOS analyzers (RM0, RM12) ran independently, operated with separate calibrations, had their own compressors, and pulled air from an inlet also servicing the flask package. This intentional delay makes it possible to observe solitary transient phenomena and bias against any platform-induced effects that should have zero delay. To assess the performances of both systems, a common gas source (cylinder on board aircraft) of known concentration was measured by both continuous analyzers for a one hour flight on 2 August 2011 (Fig. 5). Field precision of RM0 and RM12 was 0.10 ppm (standard deviation of $N = 2814$ observations) and 0.25 ppm (standard deviation of $N = 2937$ observations), respectively. Accuracy, including the specific mission calibration and

AMTD
5, 7187–7222, 2012

accuracy of delivery of reference gas, was 0.13 ppm and −0.06 ppm for RM0 and RM12, respectively. There was no sensitivity to platform motions or changes in pressure.

2.5 Data quality check

To improve confidence in the flasks observations, in 2002 we started collecting a pair of flasks either in the FT, or in the mid-PBL. Besides the usual assessment of flask conditioning and actual measurements quality control, which includes the difference between the two members of the pair (the pair was flagged if the pair difference is larger than 0.5 ppm), we also cross-referenced sampling date and time, latitude, longitude, and elevation for each individual flask. Around 5 % of the flask-measurement metadata initially reported were inconsistent with actual observation metadata and were subsequently corrected.

In 2006, we began observations with the 12-flask system. Between June 2007 and March 2011, consistency checks of our airborne observations were performed by comparing continuous measurements and flask-based observations. This process was a cross-validation between two independent systems (rather than merely a validation of one system by the other) and permitted detection of possible issues with either system. During this period, 124 RM0-based vertical profiles and 1371 flasks have been collected. Figure 6a shows the distribution of the difference between RM0 data and flask data. Across this dataset, there is no significant offset between the two systems, and the standard deviation of the difference is 0.7 ppm. The distribution of the difference has a fairly long-tail, meaning that sometimes the flask-based and RM0 observation do not compare well with each other. Timing of sample acquisition of a fluctuating atmosphere by the flask technology is probably a significant source of noise for this comparison (Fig. 6b, c). The "flushing + acquisition" window of the flasks is ten's of seconds, and fluctuations in the PBL can be large (a ppm or more) during that time interval for an aircraft flying at approximately 100 $m\,s^{-1}$ (see discussion below on observed horizontal variability).

AMTD
5, 7187–7222, 2012

As mentioned above, on 16 March 2011 RM12 was deployed on the ACME platform. RM12 showed a precision of 0.25 ppm (standard deviation of $N = 2937$ observations), due to the use of noisier earlier generation electronics. Figure 7 gives an example of observations collected using all three systems (RM0, RM12, and PFP) during an 28 April 2011 flight. The mean and standard deviation of the difference between RM0 and RM12 was 0.06 ppm and 0.3 ppm, respectively. Noise in the difference between observations from the pair of analyzers should equal the square root of the sum of the square of the accuracy of each analyzer. For thirty-seven flights between 16 March 2011 and 30 July 2011, comparisons made in the same manner gave a mean RM0–RM12 difference of −0.08 ppm and a standard deviation of the difference of 0.31 ppm. The standard deviation of the difference was largely controlled by the electro-optical noise of RM12 (Fig. 6d). The use of multiple technologies on the ACME platform (i.e. broadband validation) has improved objectivity of the airborne platform substantially by allowing detection and diagnostics of problems in all parts of the system (flask, continuous analysers, and tubing).

3 Results and discussion

3.1 Typical atmospheric CO_2 profiles

Observed mixing ratio patterns are driven by CO_2 sources and sinks and atmospheric transport (Gerbig et al., 2003; Choi et al., 2008). Flights were usually made in the afternoon (Fig. 2), when the PBL is fully developed. Vertical mixing in the PBL responds to land-surface properties such as temperature, moisture, and wind speed (Denning et al., 1995). Above the PBL, the atmosphere is usually non-turbulent and stratified, and CO_2 concentrations are influenced by large-scale circulation (Stull et al., 1988). Figure 8 shows vertical CO_2 concentration profiles collected by RM0 analyzer and flask during the descent portion of three typical flights (Fig. 8a: 18 March 2009; Fig. 8b: 20 May 2009; and Fig. 8c: 27 October 2010), using the RM0 analyzer and flask-based

AMTD
5, 7187–7222, 2012

measurements. The observed variability across any particular horizontal leg demonstrates the difficult of comparing CO_2 flask and continuous measurements. The difference between flask and RM0 observations are larger within the PBL and where large horizontal variability is observed by RM0. In addition, flask-based observations do not give information about fine scale variability in CO_2 concentrations.

During wintertime in general and for the flight described in Fig. 8a specifically, plant respiratory flux and anthropogenic emissions dominate the land-atmosphere exchanges (Pataki et al., 2007). Figure 8a shows that CO_2 concentrations in the PBL are relatively uniform around 397 ppm, while CO_2 concentrations above the PBL are 10 ppm lower. During summe and fall in general and for the flight described in Fig. 8c, vegetation photosynthesis drives the land-atmoshpere exchange (Bakwin et al., 1998). In those seasons, the vertical pattern is reversed, CO_2 concentrations in the PBL are relatively uniform around 381 ppm, while CO_2 concentrations above the PBL are 10 ppm higher. Figure 8b shows relatively uniform CO_2 concentrations from the top to the bottom of the vertical profile. May is a transition time in Northern America, with the land-surface dominance shifting from a plant respiration to a plant uptake, even if May is the month of peak uptake by regionally grown winter wheat (Riley et al., 2009), resulting in similar mole fractions above and below the PBL. Summer and fall, and winter conditions are associated with a large difference in CO_2 concentrations accross the top of the PBL ($\sim$ 2000 m). Although this fairly large gradient accross the PBL observed using continuous measurements of CO_2 from a tall tower (Helliker et al., 2004) or flasks collected from an aircraft (Williams et al., 2011) has been used to estimate net CO_2 flux, uncertainty on those estimates has not been well quantified and the use of regular continuous airborne observations could help improve estimates of flux.

3.2 Seasonal patterns

Ground-based observations in the SGP show CO_2 concentrations vary diurnally by up to 100 ppm and seasonally by $\sim$ 15 ppm, due to ecosystem exchanges with the atmosphere, proximity to fossil sources, changes in PBL depth, and exchanges with the FT

AMTD
5, 7187–7222, 2012

(Pearman et al., 1983; Enting et al., 1991; Denning et al., 1998). CO_2 seasonal cycle amplitude and trend can be estimated at different elevations using both continuous and flasks observations. Figure 9 shows continuous CO_2 observations collected using RM0 between November 2007 and July 2012. Figure 10 shows CO_2 observations collected from flasks between September 2002 and July 2012. The seasonal maximum and minimum CO_2 concentrations occur in March and August of each year, respectively, reflecting photosynthetic drawdown and terrestrial ecosystem respiration (Conway et al., 1994). The timing of the seasonal cycle is nearly the same at both heights. Over the 10-yr record, the peak-to-peak amplitude of the seasonal cycle is ∼ 15 ppm at 3000 m (FT), and ∼ 30 ppm at 1000 m (PBL) (Figs. 9 and 10). The difference in the seasonal cycle amplitude between the two height is large (∼ 15 ppm) because the seasonal amplitude of CO_2 in the PBL is amplified by the rectifier effect of seasonal variation in PBL height covarying with CO_2 sources and sinks (Denning et al., 1998). Other work has shown that covariance of atmospheric transport also contributes to the large seasonal amplitude observed in the SGP (Williams et al., 2011). CO_2 concentration trend at 3000 m estimated from RM0 observations is $\sim 1.91\ \mathrm{ppm\,yr^{-1}}$ between 2008 and 2012, very close to the Mauna Loa trend of $1.95\ \mathrm{ppm\,yr^{-1}}$ over the same period.

Although historical time series of vertical profiles give valuable information (Figs. 9 and 10), atmospheric transport modelers are usually more interested in weekly or monthly average observations rather than a particular observations or flight. A seasonal composite of vertical CO_2 concentraiton profiles between 2007 and 2011 (Fig. 11) demonstrates the regional effects of plant activity and anthropogenic sources relative to the well-mixed northern hemispheric signal recorded at Mauna Loa. The CO_2 vertical gradient between the FT and PBL is negative (∼ −7 ppm) in winter and positive (∼ 4 ppm) in summer. No vertical gradient was observed when all flights were averaged over spring. It is important to remember that Fig. 11 shows a composite of flights, meaning that individual flights occasionally had very different vertical structures as indicated by the relatively large measured standard deviation. The standard deviation is larger in the PBL than in the FT, decreasing monotonically with altitude, reflecting

AMTD
5, 7187–7222, 2012

hemispheric mixing. It remains significant (> 1 ppm) relative to the instrumental precison of 0.1 ppm, up to 5000 m (a.m.s.l.).

3.3 Horizontal variability with altitude

As described earlier, large variability in CO_2 concentrations across individual horizontal legs was commonly observed, with three implications for carbon cycle studies (Fig. 8).

First, the horizontal variability sometimes resulted in biases between flask and continuous CO_2 measurements when the flask values were compared to continuous data for the whole flight leg. In that situation, the use of instantaneous flask measurements to characterize CO_2 concentration gradients to inform atmospheric inversions of surface CO_2 exchanges may also be biased. We present several examples of CO_2 concentration heterogeneity and mean biases across seasons. To illustrate vertical and horizontal CO_2 concentration variability, we chose a single flight from 4 August 2008, a day that is typical of this time of year in the SGP, i.e. after the dominant crop (winter wheat) has senesced, the pasture is at peak productivity, and the PBL is relatively high (Fig. 12). On this afternoon, FT continuous and flask CO_2 concentrations were 384.3 ppm (stdev = 0.24 ppm) and 384.2 ppm, respectively. The continuous CO_2 concentrations had a left-skewed probability distribution and there was no significant difference between continuous and flask measurements. Within the PBL, continuous and flask CO_2 concentration means were 386.5 (stdev = 0.32 ppm with a roughly symmetric probability distribution) and 385.8 ppm, respectively. The bias between the means of the continuous and flask CO_2 mole fraction measurements was 0.7 ppm. CO_2 concentrations at the PBL top were much more variable (386.2 ppm; stdev = 0.69 ppm) with a flatter and bi-modal probability distribution, and the single flask value was 0.41 ppm lower than the mean of continuous data. Figure 13 characterizes the variability between flask and continuous data over the five years of observations by elevation. In general: (1) horizontal variability and consequent differences between continuous and flask CO_2 concentration measurements was larger in the PBL than in the FT and summer than in winter; (2) maximum variability was seen at the top of the PBL, except in spring when

AMTD
5, 7187–7222, 2012

it was maximum near the surface. We note that the horizontal leg segments of the vertical profiles are 5 and 10 min long (length ~20 km and ~40 km), above and below 2000 m, respectively, which might not capture the full extent of the regional horizontal variability.

Second, the horizontal variability had vertical and seasonal structure, with more variability at the PBL-FT interface than above or below, and more variability when there was a larger concentration gradient between PBL and FT to mix across that interface. The large heterogeneity in CO_2 concentrations near the PBL-FT interface may indicate discontinuous and sporadic exchanges across this interface and may be relevant to studies of cloud convection, subsidence and entrainment, and inversion-based inferences of surface CO_2 exchanges. Although the single-flask concentration values were usually within 0.2 ppm of the associated altitude-mean from continuous observations, the large horizontal variability indicates that transport processes may not be well represented by the use of flask observations alone. The atmospheric inversion models cited above have applied weekly-monthly averages of concentration measurements, and very often these measurements are taken relatively close to the surface. Although not a component of the analysis here, the large variability in horizontal-leg CO_2 concentrations near the PBL, more modest horizontal-leg variations in the FT, and importance of characterizing the PBL depth accurately to estimate mixed-layer CO_2 concentrations, imply that this simple characterization of the concentration gradient between the FT and PBL may be misleading.

Finally, having continuous observations allows the quantification of the error associated with the mean value for a given elevation or atmospheric layer, due to spatio-temporal variability and instrument error. Such error characterization allows quantitative error propagation in studies using these data.

AMTD
5, 7187–7222, 2012

4 Conclusions

The ten years of atmospheric CO_2 profiles presented here show the strong influence of land surface fluxes on PBL-FT gradients and how they vary seasonally, and the continental influence on the amplitude of seasonal variability in concentrations. The secular increase in FT atmospheric CO_2 mixing ratios at SGP was consistent with the trend at Mauna Loa of 1.95 ppm yr^{-1}.

There was substantial variability in CO_2 mixing ratios over the 5–10 min horizontal legs, generally largest within the PBL and smaller in the FT. A better understanding of the source of this fine-scale variability would give insight into controls on vertical transport mechanisms for atmospheric CO_2 and improve atmospheric inversions.

To test whether comparability goals have been met, for example the WMO/GAW target of < 0.1 ppm, we recommend that multiple technologies be deployed on each airborne platform. From our experience in the field, no single technology can be assumed to provide objective observations on a long-term basis. The combination of duplicate continuous instruments and flask collection gives rigorous diagnostics and a well-defined confidence level, and can be used to validate an objective sampling strategy when high precision and accuracy are required.

Acknowledgements. This research was supported by the Office of Biological and Environmental Research of the US Department of Energy under contract No. DE-AC02-05CH11231 as part of the Atmospheric Radiation Measurement Program (ARM), ARM Aerial Facility, and Terrestrial Ecosystem Science Program. AOS was supported by SBIR grants over a ten year period from the US Department of Commerce, the US Department of Energy and the National Aeronautics and Space Administration. The authors thank their colleagues for continuing support and discussion during the coffee breaks.

AMTD
5, 7187–7222, 2012

References

Abshire, J. B., Riris, H., Allan, G. R., Weaver, C. J., Mao, J. P., Sun, X., Hasselbrack, W. L., Kawa, S. R., and Biraud, S.: Pulsed airborne lidar measurements of atmospheric CO_2 column absorption, Tellus B, 62, 770–783, 2010.

Ackerman, T. P., Genio, A. D. D., Ellingson, R. G., Ferrare, R. A., Klein, S. A., McFarquhar, G. M., Lamb, P. J., Long, C. N., and Verlinde, J.: Atmospheric radiation measurement program science plan: current status and future direcitons of the ARM science program, US Department of Energy, Office of Biological and Environmental Research, Washington, D. C., 2004.

Bakwin, P. S., Tans, P. P., Hurst, D. F., and Zhao, C. L.: Measurements of carbon dioxide on very tall towers: results of the NOAA/CMDL program, Tellus B, 50, 401–415, 1998.

Bakwin, P. S., Tans, P. P., Stephens, B. B., Wofsy, S. C., Gerbig, C., and Grainger, A.: Strategies for measurement of atmospheric column means of carbon dioxide from aircraft using discrete sampling. J. Geophys. Res.-Atmos., 108, 4514, doi:10.1029/2002JD003306, 2003.

Billesbach, D. P., Fischer, M. L., Torn, M. S., and Berry, J. A.: A portable eddy covariance system for the measurement of ecosystem-atmosphere exchange of CO_2, water vapor, and energy. J. Atmos. Ocean. Tech., 21, 639–650, 2004.

Carouge, C., Rayner, P. J., Peylin, P., Bousquet, P., Chevallier, F., and Ciais, P.: What can we learn from European continuous atmospheric CO_2 measurements to quantify regional fluxes – Part 2: Sensitivity of flux accuracy to inverse setup, Atmos. Chem. Phys., 10, 3119–3129, doi:10.5194/acp-10-3119-2010, 2010.

Choi, Y. H., Vay, S. A., Vadrevu, K. P., Soja, A. J., Woo, J. H., Nolf, S. R., Sachse, G. W., Diskin, G. S., Blake, D. R., Blake, N. J., Singh, H. B., Avery, M. A., Fried, A., Pfister, L., and Fuelberg, H. E.: Characteristics of the atmospheric CO_2 signal as observed over the conterminous United States during INTEX-N A., J. Geophys. Res.-Atmos., 113, D07301, doi:10.1029/2007jd008899, 2008.

Ciais, P., Rayner, P., Chevallier, F., Bousquet, P., Logan, M., Peylin, P., and Ramonet, M.: Atmospheric inversions for estimating CO_2 fluxes: methods and perspectives, Climatic Change, 103, 69–92, 2010.

Conway, T. J., Tans, P. P., Waterman, L. S., and Thoning, K. W.: Evidence for interannual variability of the carbon-cycle from the national-oceanic-and-atmospheric-administration

AMTD
5, 7187–7222, 2012

climate-monitoring-and-diagnostics-laboratory global-air-sampling-network, J. Geophys. Res.-Atmos., 99, 22831–22855, 1994.
Denning, A. S., Fung, I. Y., and Randall, D.: Latitudinal gradient of atmospheric CO_2 due to seasonal exchange with land biota, Nature, 376, 240–243, 1995.
Denning, A. S., Randall, D. A., Collatz, G. J., and Sellers, P. J.: Simulations of terrestrial carbon metabolism and atmospheric CO_2 in a general circulation model, 2. Simulated CO_2 concentrations, Tellus B, 48, 543–567, 1996.
Enting, I. G. and Mansbridge, J. V.: Latitudinal distribution of sources and sinks of CO_2 – results of an inversion study, Tellus B, 43, 156–170, 1991.
Enting, I. G., Trudinger, C. M., and Francey, R. J.: A synthesis inversion of the concentration and Delta-C-13 of atmospheric CO_2, Tellus B, 47, 35–52, 1995.
Friedlingstein, P., Cox, P., Betts, R., Bopp, L., Von Bloh, W., W., Brovkin, V., Cadule, P., Doney, S., Eby, M., Fung, I., Bala, G., John, J., Jones, C., Joos, F., Kato, T., Kawamiya, M., Knorr, W., Lindsay, K., Matthews, H. D., Raddatz, T., Rayner, P., Reick, C., Roeckner, E., Schnitzler, K. G., Schnur, R., Strassmann, K., Weaver, A. J., Yoshikawa, C., and Zeng, N.: Climate-carbon cycle feedback analysis: results from the C4MIP model intercomparison, J. Climate, 19, 3337–3353, 2006.
Gerbig, C., Lin, J. C., Wofsy, S. C., Daube, B. C., Andrews, A. E., Stephens, B. B., Bakwin, P. S., and Grainger, C. A.: Toward constraining regional-scale fluxes of CO_2 with atmospheric observations over a continent: 1. Observed spatial variability from airborne platforms, J. Geophys. Res.-Atmos., 108, 4756, doi:10.1029/2002jd003018, 2003.
Gurney, K. R., Law, R. M., Denning, A. S., Rayner, P. J., Baker, D., Bousquet, P., Bruhwiler, L., Chen, Y. H., Ciais, P., Fan, S., Fung, I. Y., Gloor, M., Heimann, M., Higuchi, K., John, J., Maki, T., Maksyutov, S., Masarie, K., Peylin, P., Prather, M., Pak, B. C., Randerson, J., Sarmiento, J., Taguchi, S., Takahashi, T., and Yuen, C. W.: Towards robust regional estimates of CO_2 sources and sinks using atmospheric transport models, Nature, 415, 626–630, 2002.
Gurney, K. R., Law, R. M., Denning, A. S., Rayner, P. J., Pak, B. C., Baker, D., Bousquet, P., Bruhwiler, L., Chen, Y. H., Ciais, P., Fung, I. Y., Heimann, M., John, J., Maki, T., Maksyutov, S., Peylin, P., Prather, M., and Taguchi, S.: Transcom 3 inversion intercomparison: model mean results for the estimation of seasonal carbon sources and sinks, Global Biogeochem. Cy., 18, GB1010, doi:10.1029/2003GB002111, 2004.
Helliker, B. R., Berry, J. A., Betts, A. K., Bakwin, P. S., Davis, K. J., Denning, A. S., Ehleringer, J. R., Miller, J. B., Butler, M. P., and Ricciuto, D. M.: Estimates of net CO_2 flux by application

AMTD
5, 7187–7222, 2012

of equilibrium boundary layer concepts to CO_2 and water vapor measurements from a tall tower, J. Geophys. Res.-Atmos., 109, D20106, doi:10.1029/2004jd004532, 2004.
Hill, T. C., Williams, M., Woodward, F. I., and Moncrieff, J. B.: Constraining ecosystem processes from tower fluxes and atmospheric profiles, Ecol. Appl., 21, 1474–1489, 2011.
Huntzinger, D. N., Gourdji, S. M., Mueller, K. L., and Michalak, A. M.: A systematic approach for comparing modeled biospheric carbon fluxes across regional scales, Biogeosciences, 8, 1579–1593, doi:10.5194/bg-8-1579-2011, 2011.
IPCC: Climate Change 2007: The Physical Science Basis. Contribution of Working Group I to the Fourth Assessment Report of the IPCC, Cambridge University Press, Cambridge, UK and New York, 2007.
Keeling, C. D.: The concentration and isotopic abundances of carbon dioxide in the atmosphere, Tellus, 12, 200–203, 1960.
Kuai, L., Worden, J., Kulawik, S., Bowman, K., Biraud, S., Abshire, J. B., Wofsy, S. C., Natraj, V., Frankenberg, C., Wunch, D., Connor, B., Miller, C., Roehl, C., Shia, R.-L., and Yung, Y.: Profiling tropospheric CO_2 using the Aura TES and TCCON instruments, Atmos. Meas. Tech. Discuss., 5, 4495–4534, doi:10.5194/amtd-5-4495-2012, 2012.
Kulawik, S. S., Jones, D. B. A., Nassar, R., Irion, F. W., Worden, J. R., Bowman, K. W., Machida, T., Matsueda, H., Sawa, Y., Biraud, S. C., Fischer, M. L., and Jacobson, A. R.: Characterization of Tropospheric Emission Spectrometer (TES) CO_2 for carbon cycle science, Atmos. Chem. Phys., 10, 5601–5623, doi:10.5194/acp-10-5601-2010, 2010.
Kulawik, S. S., Worden, J. R., Wofsy, S. C., Biraud, S. C., Nassar, R., Jones, D. B. A., Olsen, E. T., and Osterman, G. B., and the TES and HIPPO teams: Comparison of improved Aura Tropospheric Emission Spectrometer (TES) CO_2 with HIPPO and SGP aircraft profile measurements, Atmos. Chem. Phys. Discuss., 12, 6283–6329, doi:10.5194/acpd-12-6283-2012, 2012.
Langenfelds, R. L., Francey, R. J., Steele, L. P., Spencer, D. A., and Lucarelli, M. P.: Program reports 4.10: Flask sampling from Cape Grim overflights, in Baseline Atmospheric Program (Australia) 1996, edited by: Gras, J. L., Derek, N., Tindale, N. W., and Dick, A. L., 96–97, Bur. of Meteorol. and CSIRO Atmos. Res., Melbourne, Australia, 1999.
Lin, J. C., Gerbig, C., Wofsy, S. C., Andrews, A. E., Daube, B. C., Grainger, C. A., Stephens, B. B., Bakwin, P. S., and Hollinger, D. Y.: Measuring fluxes of trace gases at regional scales by Lagrangian observations: application to the CO_2 budget and rectification airborne (COBRA) study, J. Geophys. Res.-Atmos., 109, D15304, doi:10.1029/2004JD004754, 2004.

AMTD
5, 7187–7222, 2012

Marquis, M. and Tans, P.: Climate change – carbon crucible, Science, 320, 460–461, 2008.
Masarie, K. A., Langenfelds, R. L., Allison, C. E., Conway, T. J., Dlugokencky, E. J., Francey, R. J., Novelli, P. C., Steele, L. P., Tans, P. P., Vaughn, B., and White, J. W. C.: NOAA/CSIRO flask air intercomparison experiment: a strategy for directly assessing consistency among atmospheric measurements made by independent laboratories, J. Geophys. Res.-Atmos, 106, 20445–20464, 2001.
Mays, K. L., Shepson, P. B., Stirm, B. H., Karion, A., Sweeney, C., and Gurney, K. R.: Aircraft-based measurements of the carbon footprint of Indianapolis, Environ. Sci. Technol., 43, 7816–7823, 2009.
NACP SIS: http://www.nacarbon.org/nacp/documents/NACP-SIS-final-july05.pdf (last access: 24 September 2012), 2005.
Pak, B. C., Langenfelds, R. L., Francey, R. J., Steele, L. P., and Simmonds, I.: A climatology of trace gases from the Cape Grim overflights, 1992–1995, in Baseline Atmospheric Program (Australia) 1994–1995, edited by: Francey, R. J., Dick, A. L., and Derek, N., 41–52, Bur. of Meteorol. and CSIRO Atmos. Res., Melbourne, Australia, 1996
Pales, J. C. and Keeling, C. D.: Concentration of atmospheric carbon dioxide in Hawaii, J. Geophys. Res., 70, 6053-6076, 1965.
Pataki, D. E., Xu, T., Luo, Y. Q., and Ehleringer, J. R.: Inferring biogenic and anthropogenic carbon dioxide sources across an urban to rural gradient, Oecologia, 152, 307–322, 2007.
Pearman, G. I., Hyson, P., and Fraser, P. J.: The global distribution of atmospheric carbon-dioxide.1: Aspects of observations and modeling, J. Geophys. Res.-Ocean Atmos., 88, 3581–3590, 1983.
Peters, W., Jacobson, A. R., Sweeney, C., Andrews, A. E., Conway, T. J., Hughes, J., Schaefer, K., Masarie, K. A., Jacobson, A. R., Miller, J. B., Cho, C. H., Ramonet, M., Schmidt, M., Ciattaglia, L., Apadula, F., Helta, D., Meinhardt, F., di Sarra, A. G., Piacentino, S., Sferlazzo, D., Aalto, T., Hatakka, J., Strom, J., Haszpra, L., Meijer, H. A. J., van der Laan, S., Neubert, R. E. M., Jordan, A., Rodo, X., Morgui, J. A., Vermeulen, A. T., Popa, E., Rozanski, K., Zimnoch, M., Manning, A. C., Leuenberger, M., Uglietti, C., Dolman, A. J., Ciais, P., Heimann, M., and Tans, P. P.: An atmospheric perspective on North American carbon dioxide exchange: carbontracker, Proc. Natl. Acad. Sci. USA, 104, 18925–18930, 2007.
Peters, W., Krol, M. C., van der Werf, G. R., Houweling, S., Jones, C. D., Bousquet, P., Peylin, P., Maksyutov, S., Marshall, J., Rodenbeck, C., Langenfelds, R. L., Steele, L. P., Francey, R. J., Tans, P., and Sweeney, C.: Seven years of recent European net terrestrial carbon dioxide

AMTD
5, 7187–7222, 2012

exchange constrained by atmospheric observations, Global. Change. Biol., 16, 1317–1337, 2010.
Pickett-Heaps, C. A., Rayner, P. J., Law, R. M., Ciais, P., Patra, P. K., Bousquet, P., Peylin, P., Maksyutov, S., Marshall, J., Rödenbeck, C., Langenfelds, R. L., Steele, L. P., Francey, R. J., Tans, P., and Sweeney, C.: Atmospheric CO_2 inversion validation using vertical profile measurements: analysis of four independent inversion models, J. Geophys. Res.-Atmos, 116, D12305, doi:10.1029/2010jd014887, 2011.
Rayner, P. J., Enting, I. G., Francey, R. J., and Langenfelds, R.: Reconstructing the recent carbon cycle from atmospheric CO_2, delta C-13 and O_2 / N_2 observations, Tellus B, 51, 213–232, 1999.
Rayner, P. J., Law, R. M., O'Brien, D. M., Butler, T. M., and Dilley, A. C.: Global observations of the carbon budget – 3. Initial assessment of the impact of satellite orbit, scan geometry, and cloud on measuring CO_2 from space, J. Geophys. Res.-Atmos, 107, 4557, doi:10.1029/2001JD000618, 2002.
Riley, W. J., Biraud, S. C., Torn, M. S., Fischer, M. L., Billesbach, D. P., and Berry, J. A.: Regional CO_2 and latent heat surface fluxes in the Southern Great Plains: measurements, modeling, and scaling, J. Geophys. Res.-Biogeo., 114, G04009, doi:10.1029/2009JG001003, 2009.
Shepson, P. B., Cambaliza, M., Davis, K., Gurney, K., Lauvaux, T., Richardson, N., Richardson, S., Sweeney, C., and Turnbull, J.: Indianapolis flux experiment (INFLUX): experiment design and new results regarding measurements of urban-area CO_2 and CH_4 emission fluxes, Abstr. Pap. Am. Chem. S., 242, 418-ENVR, 2011.
Stephens, B. B., Gurney, K. R., Tans, P. P., Sweeney, C., Peters, W., Bruhwiler, L., Ciais, P., Ramonet, M., Bousquet, P., Nakazawa, T., Aoki, S., Machida, T., Inoue, G., Vinnichenko, N., Lloyd, J., Jordan, A., Heimann, M., Shibistova, O., Langenfelds, R. L., Steele, L. P., Francey, R. J., and Denning, A. S.: Weak northern and strong tropical land carbon uptake from vertical profiles of atmospheric CO_2, Science, 316, 1732–1735, 2007.
Stephens, B. B., Miles, N. L., Richardson, S. J., Watt, A. S., and Davis, K. J.: Atmospheric CO_2 monitoring with single-cell NDIR-based analyzers, Atmos. Meas. Tech. Discuss., 4, 4325–4355, doi:10.5194/amtd-4-4325-2011, 2011.
Stull, R. B.: An Introduction to Boundary Layer Meteorology, Kluwer Academic, Boston, Mass, 666 pp., 1988.

AMTD
5, 7187–7222, 2012

Tans, P. P., Thoning, K. W., Elliott, W. P., and Conway, T. J.: Error-estimates of background atmospheric CO_2 patterns from weekly flask samples, J. Geophys. Res.-Atmos, 95, 14063–14070, 1990.

Williams, I. N., Riley, W. J., Torn, M. S., Berry, J. A., and Biraud, S. C.: Using boundary layer equilibrium to reduce uncertainties in transport models and CO_2 flux inversions, Atmos. Chem. Phys. Discuss., 11, 11455–11495, doi:10.5194/acpd-11-11455-2011, 2011.

WMO: Report of the 15th WMO/IAEA meeting of experts on carbon dioxide, other greenhouse gases, and related tracers measurement techniques, Jena, Germany, 2011.

Wunch, D., Toon, G. C., Wennberg, P. O., Wofsy, S. C., Stephens, B. B., Fischer, M. L., Uchino, O., Abshire, J. B., Bernath, P., Biraud, S. C., Blavier, J.-F. L., Boone, C., Bowman, K. P., Browell, E. V., Campos, T., Connor, B. J., Daube, B. C., Deutscher, N. M., Diao, M., Elkins, J. W., Gerbig, C., Gottlieb, E., Griffith, D. W. T., Hurst, D. F., Jiménez, R., Keppel-Aleks, G., Kort, E. A., Macatangay, R., Machida, T., Matsueda, H., Moore, F., Morino, I., Park, S., Robinson, J., Roehl, C. M., Sawa, Y., Sherlock, V., Sweeney, C., Tanaka, T., and Zondlo, M. A.: Calibration of the Total Carbon Column Observing Network using aircraft profile data, Atmos. Meas. Tech., 3, 1351–1362, doi:10.5194/amt-3-1351-2010, 2010.

Wunch, D., Wennberg, P. O., Toon, G. C., Connor, B. J., Fisher, B., Osterman, G. B., Frankenberg, C., Mandrake, L., O'Dell, C., Ahonen, P., Biraud, S. C., Castano, R., Cressie, N., Crisp, D., Deutscher, N. M., Eldering, A., Fisher, M. L., Griffith, D. W. T., Gunson, M., Heikkinen, P., Keppel-Aleks, G., Kyrö, E., Lindenmaier, R., Macatangay, R., Mendonca, J., Messerschmidt, J., Miller, C. E., Morino, I., Notholt, J., Oyafuso, F. A., Rettinger, M., Robinson, J., Roehl, C. M., Salawitch, R. J., Sherlock, V., Strong, K., Sussmann, R., Tanaka, T., Thompson, D. R., Uchino, O., Warneke, T., and Wofsy, S. C.: A method for evaluating bias in global measurements of CO_2 total columns from space, Atmos. Chem. Phys. Discuss., 11, 20899–20946, doi:10.5194/acpd-11-20899-2011, 2011.

Xueref-Remy, I., Messager, C., Filippi, D., Pastel, M., Nedelec, P., Ramonet, M., Paris, J. D., and Ciais, P.: Variability and budget of CO_2 in Europe: analysis of the CAATER airborne campaigns – Part 1: Observed variability, Atmos. Chem. Phys., 11, 5655–5672, doi:10.5194/acp-11-5655-2011, 2011.

AMTD
5, 7187–7222, 2012

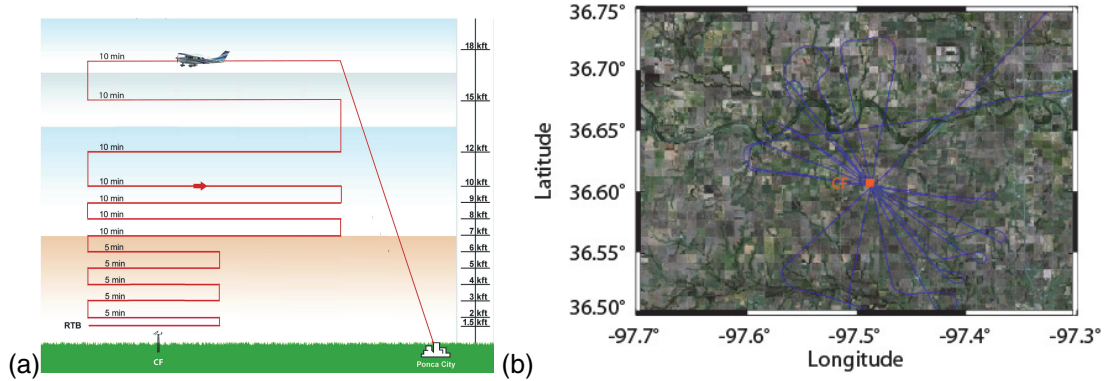

Fig. 1. (a) Vertical flight pattern for flights deployed over the ARM/SGP from 460 m to 5500 m (a.m.s.l.). **(b)** Horizontal projection of flight pattern centered on the tower of ARM/SGP, overlayed over a true color land cover picture of the region. Red square shows the location of the SGP central facility 60 m tower. Orientation of the flight pattern depends on prevailing winds and changes with altitude to avoid contamination by platform exhaust. Blue lines show the flight path for a typical flight (24 October 2011).

AMTD
5, 7187–7222, 2012

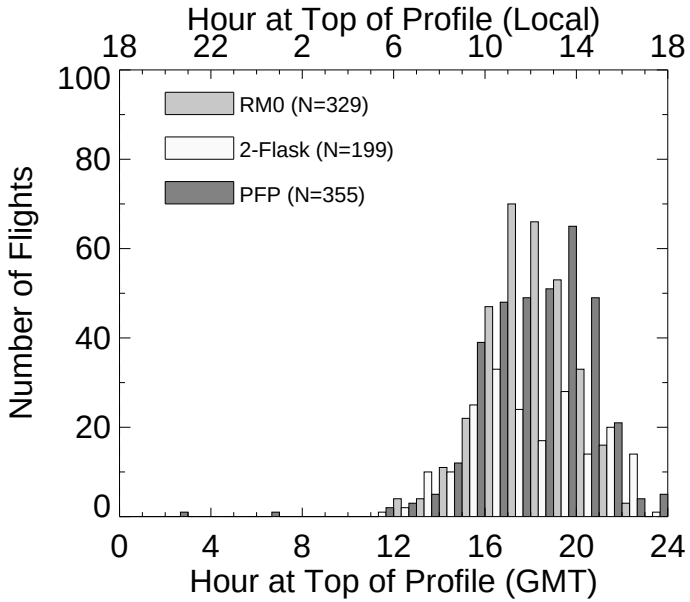

Fig. 2. Frequency histogram of hour at which highest altitude sampling took place, sorted by sampling system.

AMTD
5, 7187–7222, 2012

A multi-year record of airborne CO_2 observations

S. C. Biraud et al.

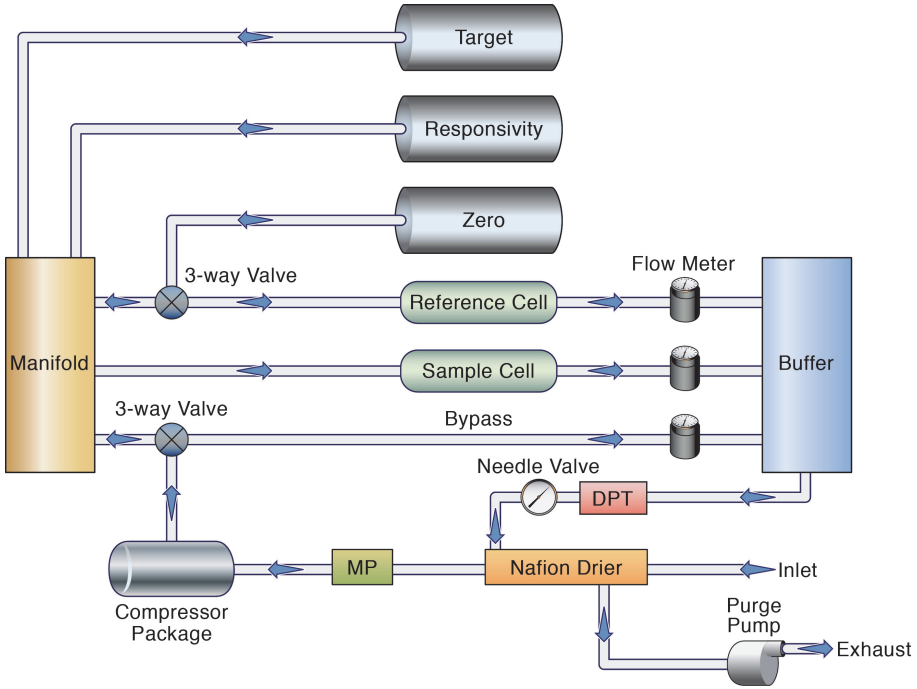

Fig. 3. Air flow for RM0 continuous analyzer.

AMTD
5, 7187–7222, 2012

A multi-year record of airborne CO_2 observations

S. C. Biraud et al.

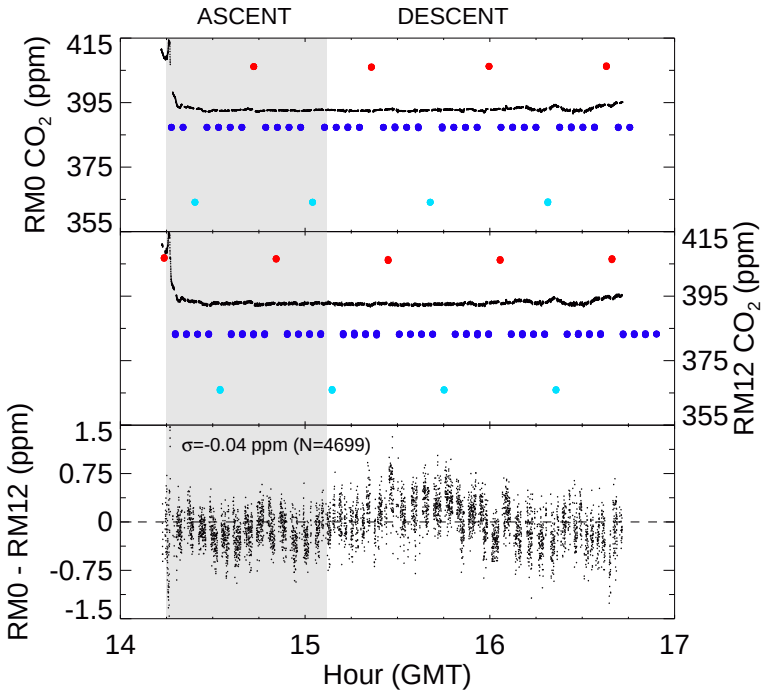

Fig. 4. CO_2 concentrations collected on 3 March 2011 by the two continuous analyzers. Top and middle panels show observations by RM0 and RM12, respectively, organized by ascent and descent. Red circles give target, dark blue circles give zero, light-blue circles give responsivity, and black dots give unknown sample measurements (1 Hz). The bottom panel shows the mean difference (0.04 ppm) between CO_2 concentrations measured using the two continuous systems.

AMTD
5, 7187–7222, 2012

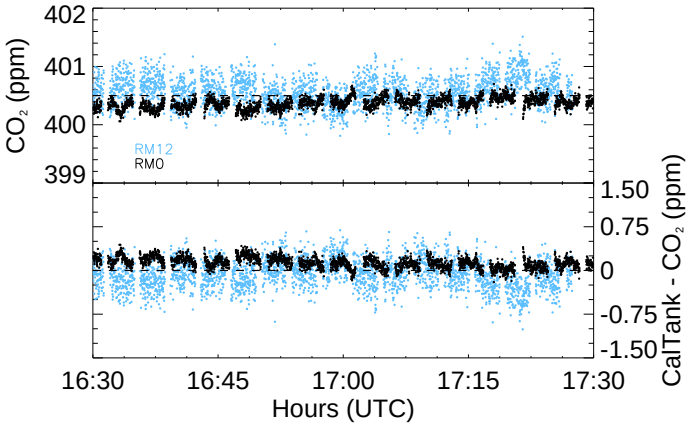

Fig. 5. In-flight accuracy and precision for the two continuous CO_2 systems (black = RM0 and blue = RM12) estimated from the measurement of CO_2 concentrations delivered by a cylinder maintained at ambient pressure and and flushed continuously by stream of reference gas calibrated earlier in the laboratory. Field precision of RM0 and RM12 as shown on top panel was 0.10 ppm (standard deviation of $N = 2814$ observations) and 0.25 ppm (standard deviation of $N = 2937$ observations), respectively. Accuracy as shown on bottom panel, including the specific mission calibration and accuracy of delivery of reference gas, was 0.13 ppm and −0.06 ppm for RM0 and RM12, respectively.

AMTD
5, 7187–7222, 2012

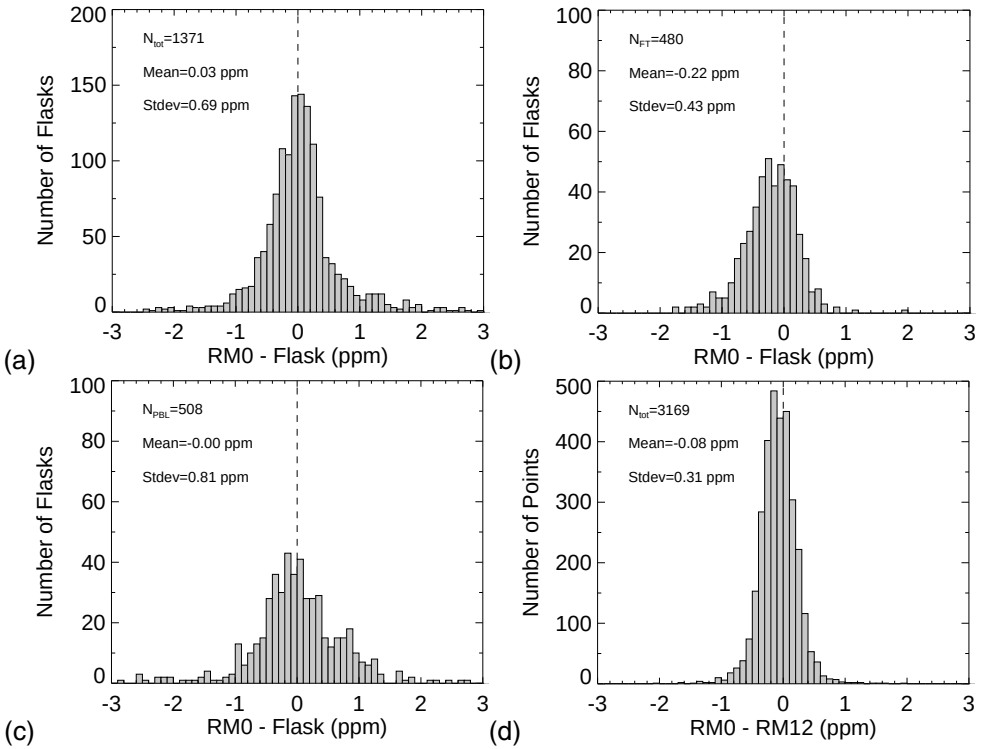

Fig. 6. Distribution of the difference calculated between: **(a)** all continuous (RM0) and flask measurements, **(b)** RM0 and flask measurements collected above 3500 m, i.e. in the FT, **(c)** RM0 and flask measurements colllected below 1000 m, i.e. within the PBL, during the November 2007 through December 2011 time period. The distribution of the difference calculated between two continuous CO_2 analyzers (RM0 and RM12) from observations collected between March 2011 and August 2011 is shown on panel **(d)**. Each point refers to the mean difference between the average signals for one of the 12 steps during descent.

AMTD
5, 7187–7222, 2012

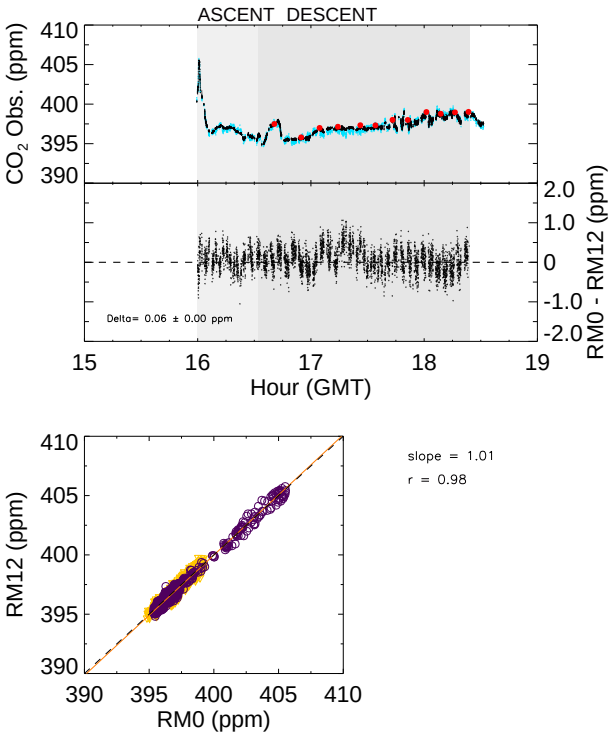

Fig. 7. CO_2 concentrations collected by broadband validation (RM0, RM12, and PFP) during an April 28, 2011 flight. The top panel shows the time series of CO_2 concentrations measured using all three systems. The middle panel shows the mean difference (0.05 ppm) between CO_2 concentrations measured using the two rack mount systems. The standard deviation of the differrence is 0.3 ppm. The botton panel shows a regression of the observations made using RM0 and RM12 systems. Open purple and yellow circles correspond to the ascent and descent parts of the flight, respectively.

AMTD
5, 7187–7222, 2012

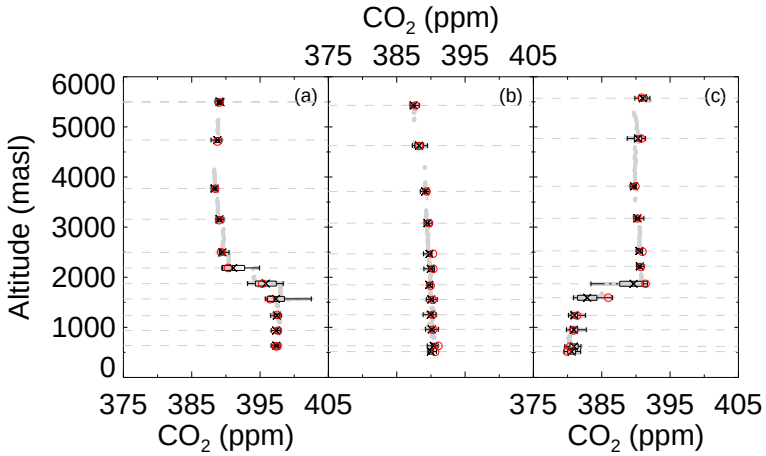

Fig. 8. Vertical profiles of CO_2 in wintertime (**a**; 18 March 2009), well-mixed condition (**b**; 20 May, 2009), and summer/fall (**c**; 27 October 2010). Gray dots shows continuous observations collected by RM0 system. CO_2 concentrations collected during horizontal legs of the flight have been binned to calculate simple statistics: minimum and maximum (black vertical segments), mean (black cross), and standard deviation (rectangle) of CO_2 concentrations. Open red circles show CO_2 concentrations measured from flasks.

AMTD
5, 7187–7222, 2012

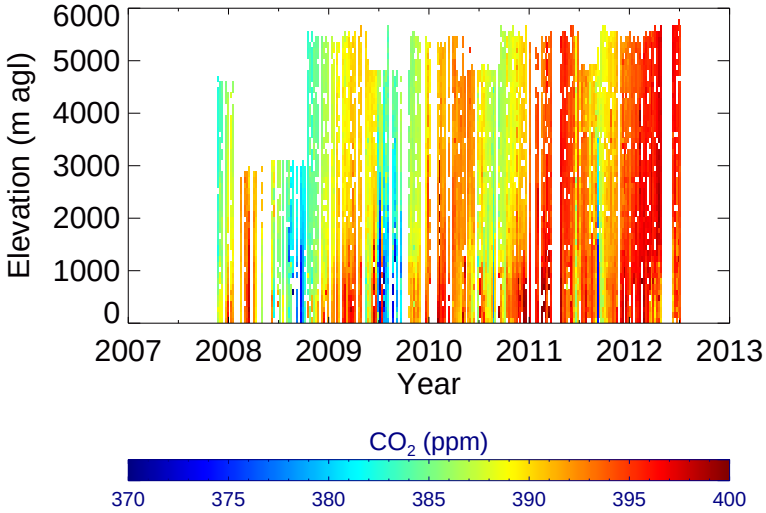

Fig. 9. Time series of continuous CO_2 vertical profiles collected from November 2007 through 31 July 2012 from RM0.

AMTD
5, 7187–7222, 2012

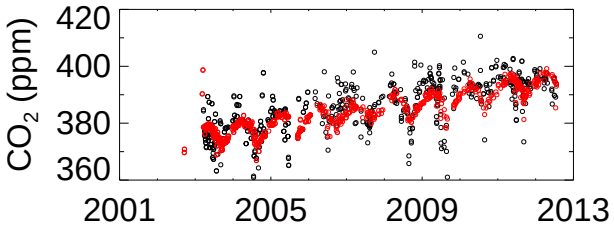

Fig. 10. Time series of CO_2 vertical profiles collected from September 2002 through July 2012 from flasks collected at 3000 m (above the PBL, red circles, $N = 740$) and 1000 m (below the PBL, black circles, $N = 604$).

AMTD
5, 7187–7222, 2012

A multi-year record of airborne CO_2 observations

S. C. Biraud et al.

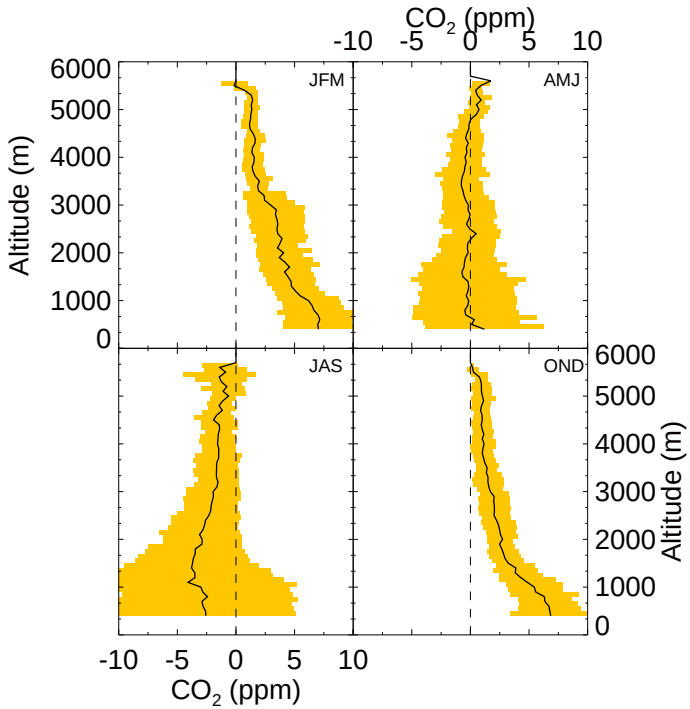

Fig. 11. Climatology of all vertical profiles collected between 2007 and 2010, shown as an anomaly relative to concentraitons at Mauna Loa (Mauna Loa data not yet available in 2011). CO_2 observations at the Mauna Loa observatory have been interpolated on a weekly basis to normalize flight profiles. CO_2 observations are binned into 100 m altitude pixel and weekly flight profiles. Each quadrant of the graph corresponds to a 3-month average climatological vertical profile (JFM: January-February-March). The solid black line shows the mean vertical profile calculated across each 3-month average, and the yellow shadded area shows one standard deviation around the average value.

AMTD
5, 7187–7222, 2012

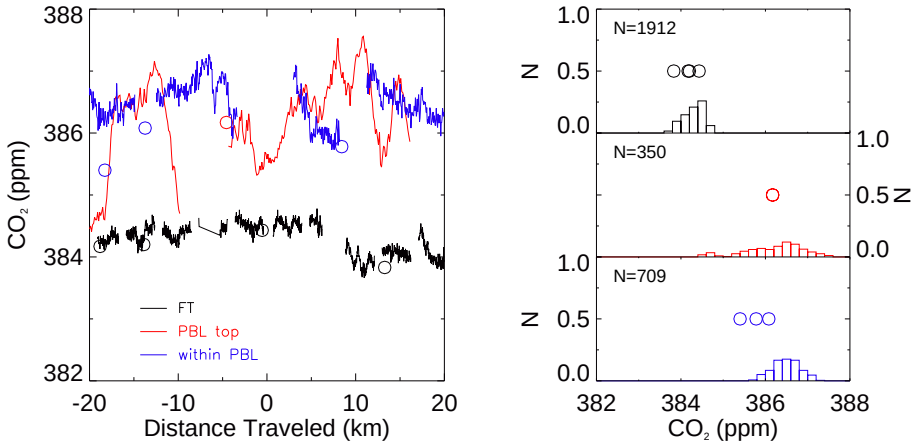

Fig. 12. (Left panel) Observed CO_2 concentrations from flasks (circles) and RM0 across horizontal legs in the FT (blue), at the PBL top (red), and within the PBL (blue), for the 4 August 2008 flight. The FT line includes observations from three horizontal legs between 2500 m and 3200 m (a.m.s.l.); the PBL top line includes observations from one horizontal leg at ~ 1000 m (a.m.s.l.); and the within PBL line includes observations from two horizontal legs between 500 m and 600 m (a.m.s.l.). The PBL legs were 5 min and are scaled to fit the same distance axis. (Right panel) The same data as in the left panel, plotted as probability distribution functions for FT, PBL top, and within PBL CO_2 concentrations. Data were non-normally distributed in the FT and at the PBL top; these types of non-normal distributions were common throughout the five years in all three altitude regimes. There was an offset, or bias, between the flask values and the mean value of the continuous data in the PBL but not in the FT.

AMTD
5, 7187–7222, 2012

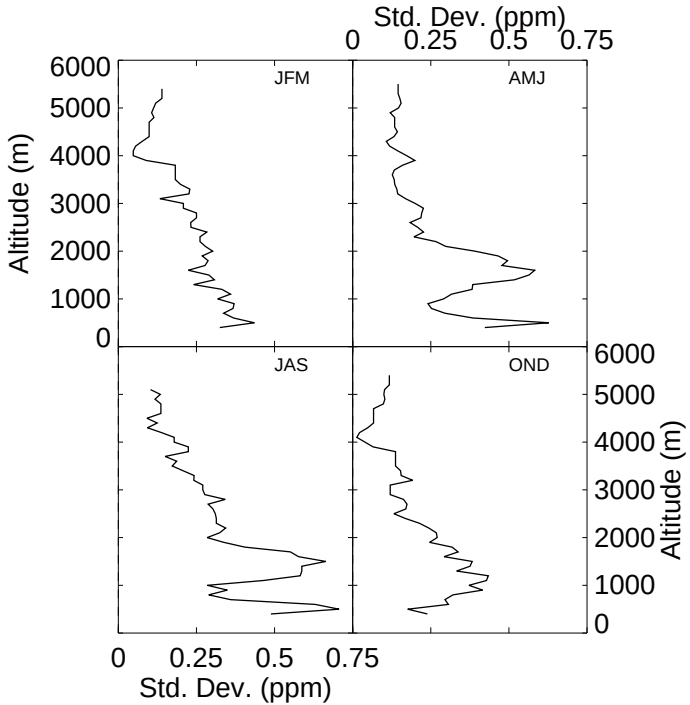

Fig. 13. The standard deviation of the differences in CO_2 concentration between RM0 and flasks collected between 2007 and 2012. The RM0 data were binned to one-minute averages. Each quadrant of the graph corresponds to a 3-month average climatological vertical profile.

AMTD
5, 7187–7222, 2012